NJC

PAPER

View Article Online
View Journal

Cite this: DOI: 10.1039/c9nj00726a

Synthesis of diarylidenecyclohexanone derivatives as potential anti-inflammatory leads against COX-2/mPGES1 and 5-LOX†

Swayamsiddha Kar, ‡[a] Gayathri Ramamoorthy, ‡[b] Shweta Sinha, [b] Meera Ramanan, [b] Jeevan Kumar Pola, [a] Nageswara Rao Golakoti, *[a] Jagadeesh Babu Nanubolu, [c] Suraj Kumar Sahoo, [a] Rajesh Babu Dandamudi [a] and Mukesh Doble *[b]

Inflammation is a pathophysiological condition which progresses through the prostaglandin (PG) and leukotriene (LT) pathways channelized by the enzymes COX/mPGES1 and 5-LOX respectively. Diarylidenecyclohexanone (DAC) derivatives (**Ia–j**, **IIa–c**, **IIIa** and **IVa**) were synthesized, characterized and screened for their *in vitro* anti-inflammatory activity *via* inhibition of 5-LOX and COX-2/mPGES1 enzymes. Compound **Ic** inhibited PGE_2 production exhibiting an IC_{50} of 6.7 ± 0.19 μM, comparable to the standard inhibitor, licofelone (IC_{50} of 5.4 ± 0.02 μM). Compounds **Ie** and **Ig** showed maximum *in vitro* inhibitory activity against 5-LOX, exhibiting an IC_{50} of 1.4 ± 0.1 μM and 1.5 ± 0.13 μM, respectively, and these are comparable to that of the standard drug, zileuton (IC_{50} = 1.2 ± 0.11 μM). **Ie** and **Ig** do not possess radical scavenging properties and may not be disrupting the redox cycle of the enzyme. Hence they may be inhibiting the enzyme by a competitive mode. One of the compounds in the DAC series (**IIc**) containing a heterocyclic thienyl ring inhibited all the three enzymes. It inhibited 5-LOX and COX-2/mPGES1 with an IC_{50} of 1.8 ± 0.12 μM and 7.5 ± 0.4 μM respectively. An RT-PCR based mRNA expression study highlighted that **Ic** predominantly inhibited the expression of COX-2 rather than mPGES1. No toxicity towards the HeLa cell line indicated that the DACs could serve as structural templates towards lead optimization of compounds for discovery of novel, potent, safe and affordable drugs as anti-inflammatory agents.

Received 11th February 2019,
Accepted 26th April 2019

DOI: 10.1039/c9nj00726a

rsc.li/njc

Introduction

When an organism has a microbial infection or tissue injury or encounters any other such conditions, a remedial strategy has been evolved wherein the immune system responds by eliminating the causes of such harmful stimuli and also brings about healing of the damaged site. The onset of such a response is inflammation. It is the primary line of defense for the organism against harmful and dangerous molecules or pathogens. Inflammation is usually seen in the form of redness, pain, swelling and heat.[1] Inflammation progresses through prostaglandin (PG) and leukotriene (LT) pathways due to the metabolism of arachidonic acid (AA). An increase in the levels of inflammatory cells including mast cells, eosinophils, neutrophils, and lymphocytes results in disorders of the respiratory tract including asthma and bronchospasm.[2–4] Leukotrienes are known to be important inflammatory mediators produced in living systems from arachidonic acid metabolism.[5,6] 5-Lipoxygenase (5-LOX) is an essential enzyme required for the production of leukotrienes from arachidonic acid. Therefore, inhibition of leukotriene biosynthesis targeting 5-LOX has been proved to be a validated strategy to treat various inflammatory infections.[7] Only one 5-LOX inhibitor, zileuton, is available commercially for the treatment of asthma,[4] but the search for other drugs targeting this enzyme with better safety and efficacy profiles still continues. PGE2 is a pro-inflammatory lipid mediator that is generated in the PG pathway through the sequential action of cyclooxygenase and mPGES1 catalysed enzymatic reactions.[8] Prolonged intake of anti-inflammatory drugs was found to be associated with GI tract disturbances (NSAIDS) and cardiovascular complications (COXIBs).[9] Similarly, over-expression of PGE2 is found in many

[a] Department of Chemistry, Sri Sathya Sai Institute of Higher Learning, PrasanthiNilayam, Andhra Pradesh, 515134, India. E-mail: gnageswararao@sssihl.edu.in; Tel: +91 9492595462
[b] Bioengineering and Drug Design Lab, Department of Biotechnology, Bhupat and Jyoti Mehta School of Biosciences, Indian Institute of Technology, Madras, Tamil Nadu, India. E-mail: mukeshd@iitm.ac.in; Tel: +91 9884691871
[c] Indian Institute of Chemical Technology (IICT), Hyderabad, India

† Electronic supplementary information (ESI) available. See DOI: 10.1039/c9nj00726a

‡ Both authors contributed equally.

chronic inflammatory diseases such as asperiodontitis,[10] diabetes,[11] and several cancers including lung, colon, prostate,[12] brain, thyroid, breast and gastrointestinal[13] types. Compounds such as licofelone and MK886 were promising candidates that blocked PGE2 production mediated by mPGES1,[12,14] where licofelone has successfully cleared phase III trials for osteoarthritis.[15] MK886 has been withdrawn due to its poor bioavailability and high levels of plasma binding. Therefore, in order to mitigate inflammation, small molecules with anti-inflammatory properties are being continuously explored.

Curcumin is a natural small molecular polyphenol. It exhibits a wide variety of pharmacological activities such as anti-cancer, anti-inflammatory, and anti-microbial.[16] Hence, curcumin is a good drug candidate with good chemotherapeutic and chemopreventive properties. But it has the disadvantage of poor stability and bioavailability because of the β-diketone moiety. So, structural changes and chemical modification are being attempted to enhance the stability and bioavailability *in vivo*.[17] One novel monocarbonyl analogue of curcumin that was found to possess anti-inflammatory activity is A13. In mice, an increase in the plasma level of NO (nitric oxide), TNF-α (tumor necrosis factor-α), and IL-6 (interleukin-6) was observed. In addition to this, A13 inhibited inflammation modulators *in vitro* and *in vivo* (Fig. 1).[18]

Apart from this, various monocarbonyl analogues of curcumin were synthesized, especially cyclopentanone analogues, and their ability to inhibit lipopolysaccharide (LPS)-induced TNF-α and IL-6 synthesis in mouse and LPS stimulated RAW 264.7 macrophages was studied.[19–21]

Diarylideneacetone, a dienone-bis-chalcone (Fig. 2C), differs from curcumin (Fig. 2A) in having only one keto group, is more symmetric than the mono-enone-chalcones (Fig. 2B) and is more stable than curcumin. The nonlinear optical properties of symmetrically substituted bis-chalcones with D–π–A–π–D type organic chromophores have earlier been reported by us.[22–24]

In an effort to explore the anti-inflammatory potential of the DACs, in this work we have undertaken the study of the anti-inflammatory properties of the DACs *via in vitro* inhibition of COX-2/mPGES1 and 5-LOX.

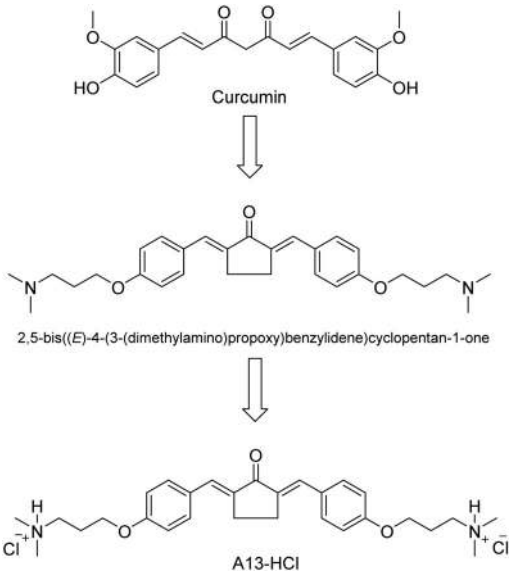

Fig. 1 Chemical structures of curcumin and A13.

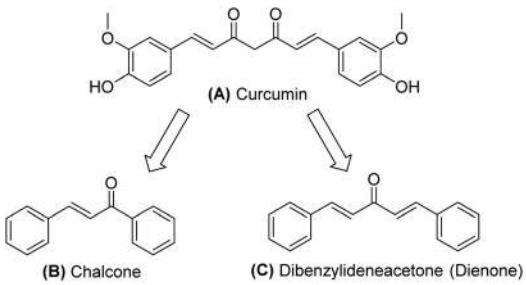

Fig. 2 Transition from dicarbonylcurcumin (A) to the two aromatic regions linked together by either an enone (B) or dienone (C).

Experimental

The various aldehydes and ketones used were obtained from S.D. Fine and Sigma-Aldrich chemicals. All solvents were distilled before use.

TNF-α was purchased from Aura Biotechnologies Private Ltd. The PGE_2 ELISA kit, licofelone, and zileuton were obtained from Cayman Chemicals. Other reagents and buffers were procured from HiMedia, India.

Synthesis

The DACs were synthesized *via* the Claisen–Schmidt condensation reaction shown in Scheme 1. The procedure in brief: in a round bottom flask ethanol (50 ml) and aqueous NaOH (10%, 50 ml) were taken. A mixture of the corresponding aryl aldehyde (0.05 mol) and cyclohexanone (0.025 mol) was prepared separately and one half of the aldehyde–ketone mixture was added to the EtOH/aq. NaOH solution with continuous stirring at room temperature. After 15 minutes, the remaining half of the aldehyde–ketone mixture was added to the round bottomed flask. The stirring of the mixture was continued till completion (checked by TLC). After completion, the contents of the round bottomed flask were poured in ice-cold water (100 ml), filtered and then washed thoroughly with ice-cold water to remove any alkali present. The solid obtained thus was dried and was recrystallized from chloroform/methanol.

In silico studies

Since we were able to grow single crystals for 2,6-bis-(3-chlorobenzylidene)-cyclohexanone (**Id**), we selected it for the *in silico* studies. The structure of **Id** was modelled using GaussView 5. The energy minimization studies for **Id** was carried out using DFT (B3LYP, 6-31G) in Gaussian 09.[25]

Cell culture and maintenance

HeLa cells (cervical cancer cell line) were procured from NCCS, Pune. The cell line was grown in DMEM containing an antibiotic solution (antimycotic 1%) and fetal bovine serum (10%).

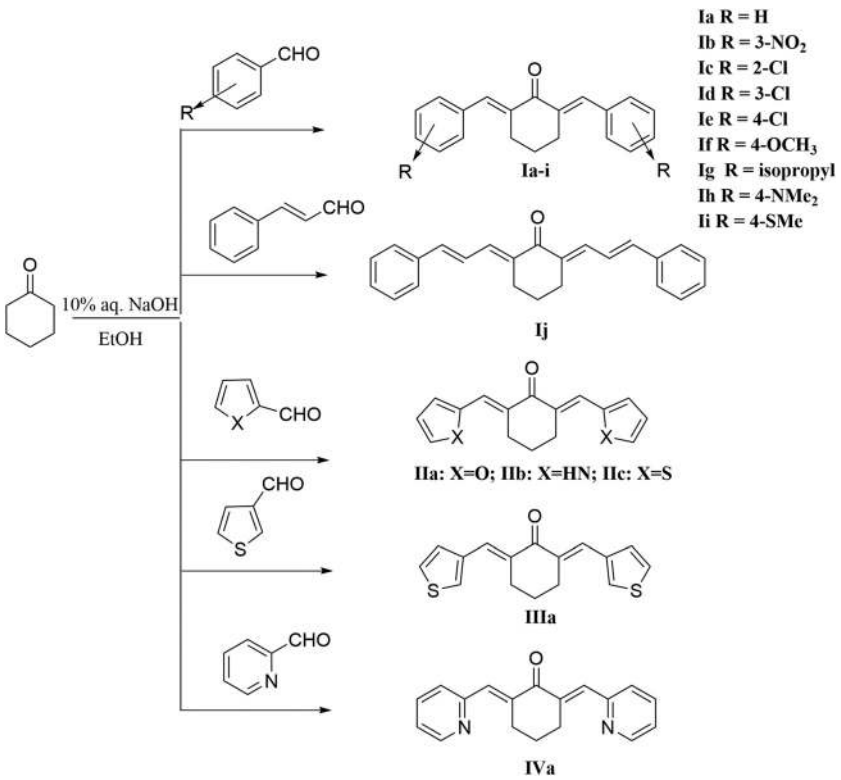

Scheme 1 Synthesis of novel diarylidenecyclohexanone derivatives.

They were maintained in a humidified atmosphere of 5% CO_2 incubated at 37 °C.

Inhibition of PGE_2 production

The cells were plated in 24-well tissue culture plates and were allowed to grow until they reached 70% confluence. TNF-α (50 ng ml^{-1}) was added to each well for 15 minutes to induce the inflammatory enzymes. The cells were then treated with a 10 μM concentration of the compounds for 24 h (for IC_{50} studies: 1, 3, and 5 till 11 μM concentrations were used). The PGE_2 released was collected from the cell culture supernatant and was added to the EIA kit (Cayman Chemical #514010). This was followed by the addition of 50 μl of antibody and 50 μl of tracer (provided in the kit). The plate was then incubated for 18 h at 4 °C. After 18 h of incubation the wells were washed five times using 200 μl of wash buffer (provided in the kit). And finally, 200 μl of Ellman's reagent was added to the wells. After 60–90 minutes the OD was measured at 405 nm using a multimode plate reader (Enspire PerkinElmer, version 4.10.3005.1440) and the pg ml^{-1} of PGE_2 produced was estimated.

mRNA expression

RNA was isolated from the HeLa cells by the TRIzol/chloroform method.[26] Then a verso cDNA synthesis kit (Thermo Scientific #AB1453A) was used to synthesize cDNA. Following that, a SYBR *Premix Ex Taq*II kit (Takara Bio, USA) was used for the analysis of gene expression with appropriate primers (Table 3) using an Eppendorf realplex PCR system. The results were standardized with human housekeeping gene, β-actin. Statistical analysis was performed with graphpad prism software (version 6.01) using one-way ANOVA by Dunnett's multiple comparisons test.

Cell viability assay

The MTT assay was carried out for analysing the cytotoxicity of the DACs.[27] HeLa cells (10^4 cells per well) were seeded in a 96-well plate. After the cells were attached, they were treated with 10 μM of compound for 24 h. Subsequently, 20 μl of MTT (3-(4,5-dimethylthiazol-2-yl)-3,5-diphenyltetrazolium bromide) was added to the cells and incubated for 4 h. After 4 h of incubation 200 μl of DMSO was added and the optical density was measured at 570 nm using a multimode plate reader (Enspire PerkinElmer, version 4.10.3005.1440).

Purification and activity assay of 5-LOX

The expression, purification and activity assay procedures for human recombinant 5-LOX were followed according to the previously reported methods.[28,29] Briefly, pT3-5-LOX plasmid transformation in *E. coli* BL21 bacteria was induced with 0.5 mM of isopropyl-D-thiogalactopyranoside for protein expression at 37 °C. The cells were lysed and sonicated in 50 mM of triethanolamine/HCl (pH 8.0), 5 mM ethylenediaminetetraacetic acid (EDTA), 60 μg ml^{-1} trypsin inhibitor, 1 mM phenylmethylsulphonylfluoride (PMSF) and 500 μg ml^{-1} lysozyme. The homogenate precipitated with ammonium sulphate was centrifuged at 16 000 × *g* at 4 °C for 30 min (Centrifuge 5418 R, Eppendorf AG) and the protein was immediately used for 5-LOX activity assays. The activity was checked using time course measurements at 236 nm (Jasco V-550 UV-vis spectrophotometer) in the presence and absence of

the test compounds. A 5-LOX protein aliquot was diluted with HEPES 2-[4-(2-hydroxyethyl)piperazin-1-yl] ethanesulfonic acid (pH 7.3) buffer containing EDTA (0.4 M), $CaCl_2$ (10 mM), and 4 mM adenosine 5′-triphosphate (ATP) and the reaction was initiated by addition of the substrate (30 μM). The amount of 5-HPETE product formed was used to determine the enzyme activity. Zileuton was used as the positive control.

DPPH radical scavenging analysis

The antioxidant properties were analysed using the stable free radical 2,2-diphenyl-1-picrylhydrazyl (DPPH) as per the previously reported method.[30] Briefly, 0.1 mM DPPH (in methanol) and 10 μM of the test compounds (in DMSO) were mixed and incubated in the dark for 30 min at room temperature and the absorbance was measured at 517 nm using a Multimode Plate reader (Enspire PerkinElmer, version 4.10.3005.1440) to determine the radical scavenging properties. Ascorbic acid was used as the positive control.

Results and discussion

Synthesis

Diarylidenecyclohexanone derivatives (**Ia–j**, **IIa–c** and **IIIa–b**) were synthesized by base catalysed Claisen–Schmidt condensation using substituted aryl aldehydes and cyclohexanone, as outlined below (Scheme 1).

Characterisation

The compounds were purified by recrystallization and characterized by UV-vis, FT-IR, ^{1}H-NMR, ^{13}C-NMR and mass spectroscopy (supplementary data provided). The UV-vis spectra for all compounds showed two bands in the region ∼250 and 380 nm. The presence of C═O (1640–1670 cm^{-1}), C═C (1600–1635 cm^{-1}), aromatic groups (two bands in the region 1450–1600 cm^{-1} and aromatic C–H out of plane bending at 900–650 cm^{-1}) and the cyclohexanone ring (C–H stretch 2850–2950 cm^{-1}) was observed in FT-IR. ^{1}H-NMR spectra also confirmed the cyclohexanone ring at ∼δ 1.88 ppm (2H, quintet) and ∼δ 2.9 ppm (4H, triplet). The β proton of the α–β unsaturated ketone was seen as a singlet at ∼δ 7.5 ppm in all the compounds, and the aromatic proton signals were in the region δ 6.6–7.5 ppm. ^{13}C-NMR signals for aromatic carbons were seen between δ 120 ppm and 160 ppm. A signal at ∼δ 190 ppm in ^{13}C-NMR was seen for the C═O group. The mass spectra of all these compounds showed the expected molecular ions confirming their structures.

The IR bands at 1521 and 1325 cm^{-1} seen in **Ib** are due to the asymmetric and symmetric stretch of $-NO_2$. The C–Cl stretch is characterized by the presence of bands at 1052 and 1066 cm^{-1} respectively for 2-Cl (**Ic**) and 3-Cl (**Id**). However, it is observed at a higher wave number of 1091 cm^{-1} in the case of 4-Cl (**Ie**) because of conjugation with the carbonyl group. In the ^{1}H NMR spectrum of the cinnamyl derivative **Ij**, the six olefinic proton signals are seen at δ 6.97 ppm (d, 2H, J = 15.6 Hz), δ 7.07 ppm (t, 2H) and δ 7.50 ppm (2H). The alkene carbons gave corresponding signals at δ 136.34 ppm, δ 123.68 ppm and δ 140.78 ppm in the ^{13}C NMR spectrum of **Ij**. In the mass spectra of thienylidene cyclohexanones **IIc** and **IIIa**, m/z: 287 $[M + H]^+$ and 288 $[M + 2]^+$ peaks were observed. This is characteristic of sulphur containing compounds. Complete spectral data along with assignments are given in the ESI.†

X-ray diffraction analysis of single crystals of 2,6-bis-(3-chlorobenzylidene)-cyclohexanone (Id)

Crystal growth. The crystal growth of 2,6-bis-(3-chlorobenzylidene) cyclohexanone (**Id**) was done by slow evaporation growth technique at ambient temperature. The purified compound was used for growing single crystals using a chloroform/ethanol mixture (1 : 1, v/v). Fig. 3 shows the ORTEP diagram and the packing obtained from the single crystal XRD studies.

Crystal structure determination. A Bruker Smart Apex CCD diffractometer was used to collect the X-ray data for the compound with graphite monochromated Mo-Kα radiation (λ = 0.71073 Å)

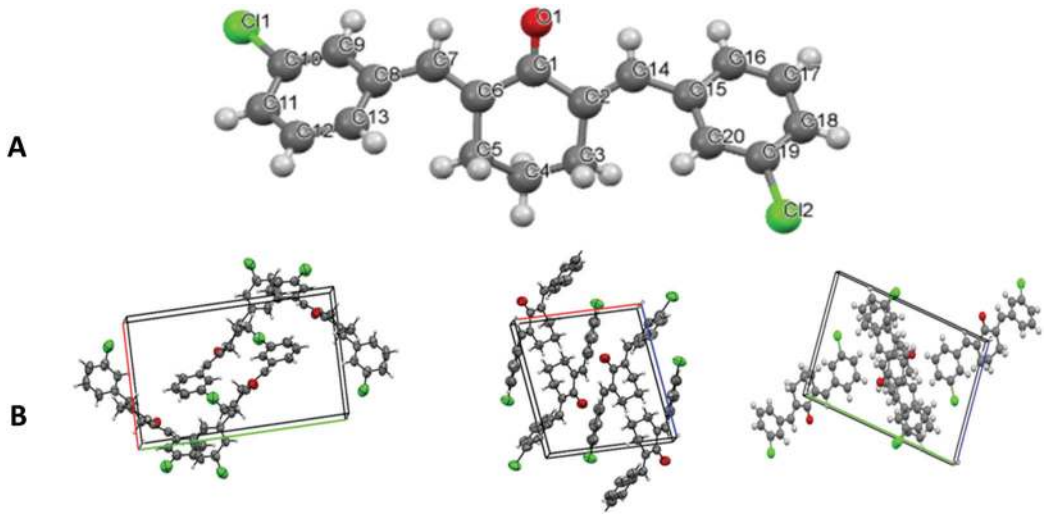

Fig. 3 2,6-Bis(3-chlorobenzylidene) cyclohexanone (**Id**): (A) ORTEP diagram with the atom-numbering scheme and (B) crystal packing diagram.

employing the ω-scan method.[31] Using four sets of frames, the preliminary lattice parameters and orientation matrices were obtained. 5397 reflections were used to determine the unit cell dimensions. The SAINT program[31] was employed for the integration and scaling of intensity data. SHELXS97[32] was used to decipher the structure of the compound by using direct methods. The refinement was obtained by the full-matrix least-squares technique available in SHELXL-2014/7.[32] For all the non-hydrogen atoms anisotropic displacement parameters were incorporated. Geometrical positioning for all the hydrogen atoms was used. Hydrogen atoms were treated as riding on their parent C atoms with C–H bond lengths of 0.93–0.97 Å and with U_{iso} (H) = 1.2U_{eq} (C) or 1.5U_{eq} for the methyl groups.

Crystal data for AU21: C20H16O1Cl2, M = 343.23.34, 0.21 × 0.16 × 0.14 mm^3, monoclinic, space group $P21/n$ (no. 14), a = 9.3742(8), b = 16.9440(15), c = 10.5608(9) Å, β = 96.730(1)°, V = 1665.9(2) Å^3, Z = 4, D_c = 1.368 g cm^{-3}, $F000$ = 712, CCD area detector, MoKα radiation, λ = 0.71073 Å, T = 293(2) K, $2\theta_{max}$ = 52.5°, 15 493 reflections collected, 3356 unique (R_{int} = 0.022), final GooF = 1.04, R_1 = 0.0506, wR_2 = 0.1326, R indices based on 2663 reflections with $I > 2\sigma(I)$ (refinement on F_2), 208 parameters, μ = 0.391 mm^{-1}, min and max resd. dens. = −0.32 and 0.39 e Å^{-3}. CCDC 1856373.†

In silico studies

The bond angles and bond lengths obtained from the single crystal XRD experiment and the Gaussian calculations were compared in order to establish the soundness of the chosen theory and basis set for the calculations. The two are summarized in Table S1a and b in the ESI.† The regression analysis of the comparison between the experimental XRD data and the simulated Gaussian data returned a significant r^2 of 0.9849 in the case of the bond lengths. Similarly, we recorded an r^2 of 0.985 in the case of the bond angles. These high coefficients indicate that the minimized conformation of the Gaussian structure aligns with the synthesised XRD structure and can be observed in Fig. 4 given below. This proves the accuracy of the chosen Gaussian basis set and level of theory and the soundness of our computed values.

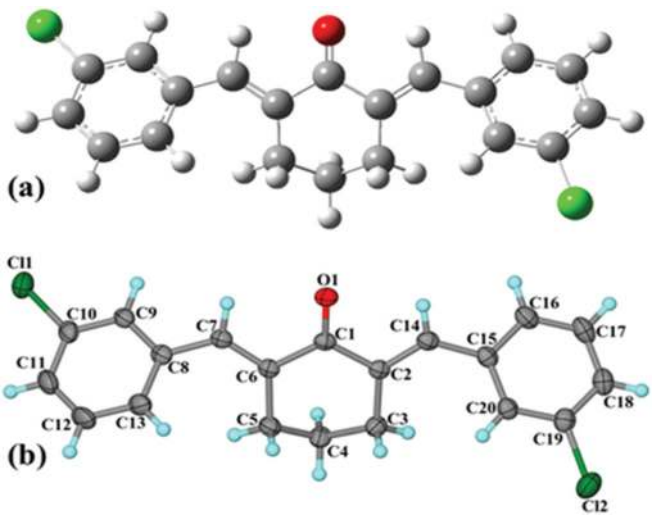

Fig. 4 2,6-Bis(3-chlorobenzylidene) cyclohexanone (**Id**): (a) Gaussian minimized structure and (b) XRD structure.

In vitro screening of anti-inflammatory activity

The results from the *in vitro* screening of the 15 DACs at 10 μM inhibiting the production of TNF-α induced PGE_2 production by HeLa cells and 5-LOX inhibition are tabulated in Table 2. From the results it is evident that the DACs do not inhibit PGE_2 and 5-LOX equally. For example, **Ic** has the best potency against PGE_2 (89.6 ± 1.7% inhibition) whereas it has lesser potency against 5-LOX (66.4% inhibition). Similarly, **Ie** has much less potency against PGE_2 (26.6 ± 3.8% inhibition) whereas it is one of the most potent molecules against 5-LOX (88.5% inhibition). Overall, among the two types of studies the DACs have greater potency against 5-LOX as a whole class because of the number of molecules showing potent activity as compared to the standard used.

Inhibition of PGE_2 production by COX-2/mPGES1

High levels of PGE_2 synthase expression are observed in the HeLa and A549 cancer cell lines.[27] Hence, the HeLa cell line was selected for this study. In the series, all the compounds exhibit good inhibitory activity towards COX-2/mPGES1 derived PGE_2 production. As mentioned earlier, **Ic** (containing *ortho* chloro) is the most potent molecule against PGE_2 with 89.6 ± 1.7% inhibition at 10 μM and has an IC_{50} value of 6.7 ± 0.2 μM. It has been reported that an *ortho*-chlorobenzyl substituted compound showed an IC_{50} around 20.5 μM against A549 cells and 0.1 μM in cell free assay.[33] The presence of a chlorine atom in lumiracoxib (a COX-2 inhibitor) shows a contributing role for selectivity of the COX-2 inhibition and this atom binds with small hydrophobic pockets (Ser-530, Val-349, Leu-531 and Ala-527).[34] Also the chloro groups enhanced the potency towards mPGES.[35] It has also been reported earlier that a chloro substituted phenyl ring in the *ortho* position exhibited better anti-inflammatory activity than di-substituted and *meta* substituted compounds.[36] And it was also observed that replacement of chlorine by methoxy, bromo and fluoro groups drastically impaired COX inhibition.[37] Thus, in line with the literature we observe the importance of the presence of the chloro group in the *ortho* position in our work also.

Over 15 derivatives have been studied against PGE_2, thus paving the way to understand the effect of structure on the activity. **Ia** is the parent compound or the simplest DAC and it has a potency of 45.3 ± 2.5% inhibition only. Among the substituted DACs we see a definitive change in activity based on the position of the substituent. It is interesting to note that **Ic**, **Id**, and **Ie** are structural isomers, but the difference in the activity brings out the importance of the position of the substituent. It is evident that substitution at the *ortho* position (**Ic**) improves the activity. On the other hand, *meta* and *para* substitutions reduced the activity. The *ortho*-chloro in the aromatic residue is more potent than the *para*-chloro group due to its better hydrophobic interaction against human isolated mPGES1 from HeLa.[38] Among the *para* substitutions it is evident that an electron pumping group increased the activity (inhibition potency of **If** > **Ig** > **Ie**). On the other hand, we have

Table 1 IC_{50} values of the best active compounds

Compound code	COX-2/mPGES1 inhibition, IC_{50} (μM)
Ic	6.7 ± 0.19
IIc	7.5 ± 0.4
Licofelone	5.4 ± 0.02

Ii which doesn't show any activity at all. **Ij** is a class apart from the other DACs due to the presence of the extended conjugation in the structure. As compared to **Ia** it has improved activity, which might be due to the presence of the extra double bonds. On similar lines we have found in the literature that the 3-phenylprop-2-en-1-one substituted compound with extended conjugation inhibits PGE_2 (95%) and COX-2 (20%) against LPS/IFN-γ induced RAW264.7 at 25 μM.[39]

Moving on to the heterocyclic DACs, it is clear that the presence of heterocycles (**IIa**, **IIb** and **IIc**) increased the PGE_2 inhibition potency as compared to the simple aromatic DAC **Ia**. Among the three heterocyclic DACs **IIc** has the highest potency (81.8 ± 3.5% inhibition) showing that the thienyl group enhances the activity. It has an IC_{50} value of 7.5 ± 0.4 μM. In the literature, a thiophen-2-yl methylene containing compound showed 87.4% ± 11.0 and 72.0% ± 7.109 inhibition against COX-2 and COX-1 at 10 μM respectively in human whole blood (HWB) assay.[40] Similarly a compound with a thiophene group (DuP-697) inhibited 80% and 85% of VEGF-induced PGE_2 production at 10 nM in human cultured umbilical vein endothelial cells (HUVECs).[41] These instances from the literature reinforce the importance of the presence of the thienyl ring, which is essential for PGE_2 inhibition. **IIc** is followed by **IIb** (68.7 ± 1.4%) and **IIa** (52. 2 ± 11.0%). This kind of significant activity of the five membered heterocyclic rings thiophene, pyrrole and furan against COX-2 at very low μM concentration has already been observed.[34] The IC_{50} values for the inhibition of PGE_2 production by COX-2/mPGES1 of the best compounds have been tabulated below in Table 1.

The SAR in PGE_2 was interesting and concluded with three outcomes. One, the substituent at the *ortho* position improves the activity. Two, an electron pumping substituent improves the activity at the *para* position. Three, heterocycles improve the activity with the thienyl group having the highest potency.

mRNA expression

The COX-1, COX-2 and mPGES1 mRNA expression levels were found by real time-PCR analysis (Table 3). TNF-α can induce mPGES1 production with or without COX-2 induction in several types of cells.[42] The result shows that 15 minutes of treatment of TNF-α induced a higher COX-2 (7.3 fold) level in comparison to the mPGES1 level (1.4 fold) (Fig. 5). Compound **IIc** decreases the COX-2 and mPGES-1 expression level from 7.3 and 1.4 fold to 1.4 and 0.7 fold respectively. Similarly, compound **Ic** decreases the COX-2 and mPGES1 expression level to 0.3 and 0.6 fold from 7.3 and 1.4 fold. These results indicate that thiophene-2-ylmethylidene and chlorobenzylidene with a cyclohexanone group strongly inhibit the prostaglandin pathway by acting predominantly on COX-2 and to some extent on mPGES1.

Inhibition of enzyme 5-LOX

The highlight of the 5-LOX study is that three of the DACs (**Ie** (88.5%), **Ig** (88.5%), and **IIc** (86.7%)) showed greater potency *in vitro* as compared to zileuton (85.6%), which is a known drug against asthma. Another DAC **IIb** showed comparable inhibition

Table 3 Primer used for RT-PCR (ESI)

β Actin	Forward: 5′CTCACCATGGATGATGATATCGC-3′ Reverse: 5′AGGAATCCTTCTGACCATGC-3′
COX-1	Forward: 5′GCTATTCCGGCCCCAACT-3′ Reverse: 5′GATGAAGGTGGCATTGACAAACT-3′
COX-2	Forward: 5′TATACTAGAGCCCTTCCTCCTGTGCC-3′ Reverse: 5′ACATCGCATACTCTGTTGTGTTCCC-3′
mPGES-1	Forward: 5′GGAACGACATGGAGACCATCTAC-3′ Reverse: 5′TCCAGGCGACAAAAGGGTTA-3′

Table 2 *In vitro* anti-inflammatory activity and cytotoxicity of the DAC derivatives

	% Inhibition (at 10 μM)		
Compounds	Inhibition of PGE_2 production	5-LOX inhibition	% HeLa cell proliferation (at 10 μM)
Ia (R═H)	45.3 ± 2.5	29.5 ± 3.0	109.9 ± 8.3
Ib (R═3-NO_2)	6.6 ± 7.7	66.0 ± 3.3	66.1 ± 6.2
Ic (R═2-Cl)	89.6 ± 1.7	66.4 ± 3.0	106.5 ± 5.5
Id (R═3-Cl)	42.8 ± 6.2	75.6 ± 1.6	74.0 ± 9.9
Ie (R═4-Cl)	26.6 ± 3.8	88.5 ± 7.0	88.2 ± 7.2
If (R═4-O-Me)	45.3 ± 9.4	51.6 ± 3.0	117.3 ± 6.2
Ig (R ═4-isopr)	34.1 ± 7.7	88.5 ± 1.00	73.8 ± 6.8
Ih (R═4-NMe_2)	54.0 ± 7.3	19.7 ± 5.9	74.1 ± 6.0
Ii (R═4-S-Me)	0.00	53.5 ± 1.0	85.6 ± 8.3
Ij (2,6-bis-cinnamylidenecyclohexanone)	67.4 ± 2.1	66.4 ± 1.0	91.8 ± 7.0
IIa (X═O)	52.2 ± 11.0	36.9 ± 1.3	90.2 ± 0.8
IIb (X═NH)	68.7 ± 1.4	83.0 ± 6.0	73.4 ± 1.8
IIc (X═S)	81.8 ± 3.5	86.7 ± 4.01	78.4 ± 10.3
IIIa (X═S)	73.2 ± 4.0	25.5 ± 2.6	69.8 ± 1.6
IVa (X═N)	57.5 ± 0.8	10.4 ± 4.6	106.0 ± 8.3
Zileuton	—	85.6 ± 1.3	—
Licofelone	98.8 ± 4.2	—	—
5-Fluorouracil	—	—	76.9 ± 3.2

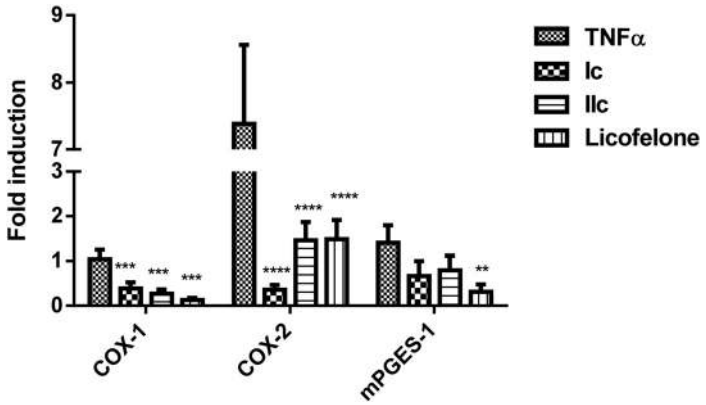

Fig. 5 mRNA expression levels of inflammatory enzymes (COX-1, COX-2 and mPGES-1) in the cyclooxygenase pathway. ** indicates p values ≤ 0.01, *** denotes p values ≤ 0.001 and **** indicates p values ≤ 0.0001 with respect to TNFα.

Table 4 IC_{50} values of the best active compounds

Compound code	5-LOX inhibition, IC_{50} (μM)
Ie	1.4 ± 0.1
Ig	1.5 ± 0.13
IIc	1.8 ± 0.12
Zileuton	1.2 ± 0.11

(83.0%) with respect to the standard. The simple DAC **Ia** has an inhibition of 29.5% only. In this case it appears that substituents at the *para* position improve the activity. Both **Ie** and **Ig** have a potency of 88.5%. Among the *para* substitutions, it appears that an electron pumping group reduces the potency; **Ih** with the 4-NMe_2 substitution has 19.7% inhibition (least among all the *para* substituted DACs). Here too we can see the effect of the position of the substituents when **Ic**, **Id** and **Ie** are compared. **Ie** with *para* substitution has the highest activity (88.51%) followed by **Id** (75.6%, *meta* substitution) and **Ic** (66.4%, *ortho* substitution). **Ib** and **Id** have *meta* substitution, but it appears that $-NO_2$ substitution in **Ib** reduces the activity (66.0%) as compared to –Cl substitution in **Id** (75.6%).

Moving to the heterocycle containing DACs, it is evident here also that heterocycles improve the activity as compared to the simple aryl DACs. As observed earlier in the case of PGE_2 inhibition, here too the thienyl DAC (**IIc**) has the highest potency (88.5%) followed by **IIb** (83.0%) and then **IIa** (36.9%); interestingly the trend remains the same in both cases. We further have a comparison between **IIc** and **IIIa**, where both have the thienyl ring. The difference in the potency (**IIc** – 88.5% and **IIIa** – 25.5%) clearly shows the importance of the position of the attachment. **IIc** was obtained from 2-thienyl carboxaldehyde whereas **IIIa** was obtained from 3-thienyl carboxaldehyde. The one third reduction in potency is a clear indication of the fact that the position of the attachment matters. In another

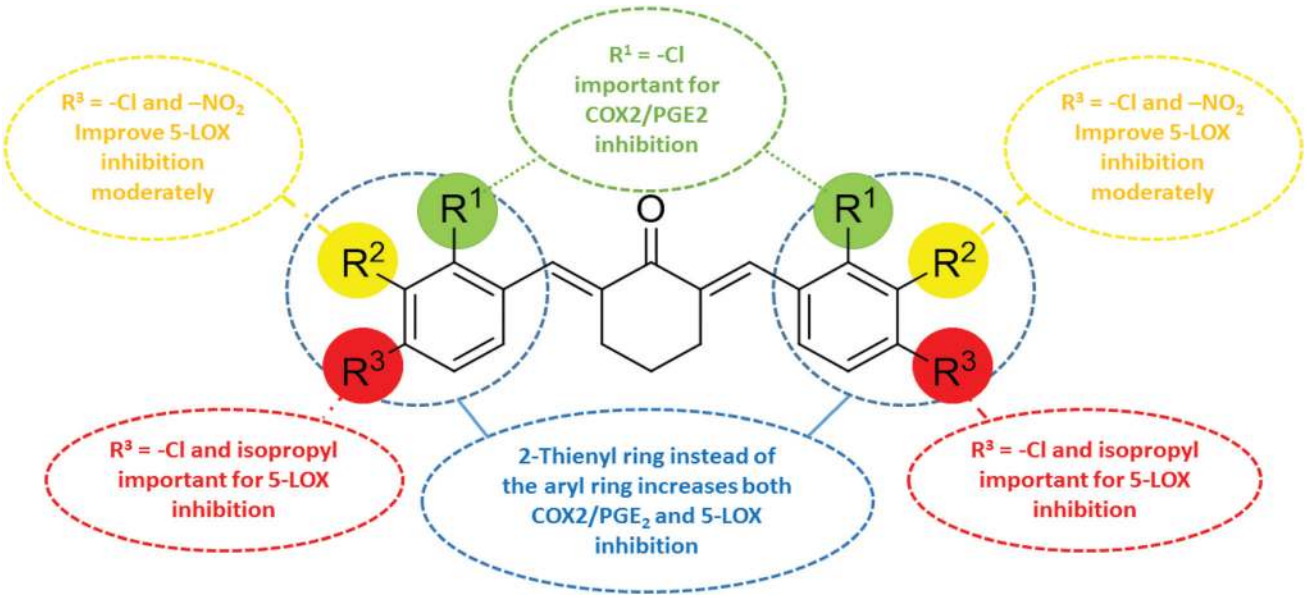

Fig. 6 Structure–activity relationship expressed diagramatically.

Table 5 DPPH radical scavenging activity

Compound code	% DPPH radical scavenging activity ± SD (10 μM)
Ie	3.19 ± 0.13
Ig	2.70 ± 0.42
IIc	3.45 ± 0.53
Ascorbic acid	46 ± 1.06

comparison we have **IIb** and **IVa** where the heterocycles have an N-atom in them. The difference being in **IIb** we have a pyrrole system whereas in **IVa** we have a pyridine system. There is a reduction of potency by 8 times from **IIb** (83.0%) to **IVa** (10.4%). This observation brings us to the conclusion that five membered heterocycles have better potency as compared to six membered heterocycles.

From the SAR studies towards 5-LOX inhibition, the following points were observed: first, three DACs (**Ie**, **Ig** and **IIc**) showed potent activity (IC_{50} of 1.4 ± 0.1, 1.5 ± 0.13 and 1.8 ± 0.12 μM respectively) with comparable activity as compared to the standard zileuton (IC_{50} of 1.2 ± 0.11 μM). Second, substituents at the *para* position have better activity but an electron pumping group at the *para* position reduces the potency. Third, heterocycles increase the potency but are limited to five membered rings and attachment at the 2nd position (use of 2-caboxaldehyde). The IC_{50} values of the best active compounds have been tabulated below in Table 4.

The overall structure–activity relationship has been summarized in Fig. 6 given above.

Radical scavenging activity

5-LOX is an enzyme which contains ''non-heme'' iron as the Fe^{3+} metal ion in its activated state. Reduction or a change in the active state of the metal is one of the mechanisms of inhibition of the enzyme by a redox type inhibitor.[43,44] Previous reports have also indicated that inhibitors which are radical scavengers may inhibit the enzyme by affecting the oxidation state of the metal and may not be selective.[27] Therefore, the DPPH radical scavenging properties of the compounds have been analysed by a previously reported method[30] and tabulated below in Table 5.

Most of the compounds in this series did not show any radical scavenging activity. The compounds **Ie**, **If** and **IIc** exhibited DPPH radical scavenging antioxidant activity below ≤5% at a 10 μM concentration. Hence it could be suggested that these compounds act on the 5-LOX enzyme as competitive inhibition and may not disrupt the redox cycle of the enzyme.

All the compounds favored HeLa cell proliferation, which is an indication that they are not toxic towards them. This is desirable because given their potent activity, they themselves are not harmful towards healthy cells and hence can be explored as new potential leads as anti-inflammatory agents.

Conclusion

In conclusion, we demonstrated the potential of diarylidenecyclohexanones as new pharmacophores for anti-inflammatory activities with **Ic** exhibiting 89.6 ± 1.7% inhibition against PGE_2. This investigation on PGE_2 inhibition led to the rationale of the structure activity relationship. The key factors to enhance the activity include substituents at the *ortho* position, an electron pumping substituent at the *para* position and heterocycles with the thienyl group. **Ic** and **IIc** significantly reduced the end product (PGE_2) of the cyclooxygenase pathway. This reiterated the role of thiophene and chloro groups and their position in reducing the anti-inflammatory enzyme in the HeLa cancer cell line, confirming their promise as anti-inflammatory leads.

Further, we identified DACs with *p*-chloro, isopropyl and thienyl substitution in **Ie** (IC_{50} of 1.4 ± 0.1 μM), **Ig** (IC_{50} of 1.5 ± 0.13 μM) and **IIc** (IC_{50} of 1.8 ± 0.12 μM) respectively as potent derivatives against enzyme 5-LOX as compared to zileuton. This establishes that the electronegative groups and donating groups at the *para* position favor the inhibition of 5-LOX, while in heterocyclic DACs, the substitution with five membered ring systems (thiophene and pyrrole) at the 2nd position favored 5-LOX inhibition. Overall, the heterocyclic thienyl DAC **IIc** demonstrated dual inhibition against both 5-LOX and PGE_2 (86.7 ± 4.0 and 81.8 ± 3.5% respectively). In essence, this study establishes that diarylidenecyclohexanones can be explored as good anti-inflammatory pharmacophores for future design of drugs given the selective high potency against PGE_2 and 5-LOX without toxicity towards healthy human cells.

Conflicts of interest

There are no conflicts to declare.

Acknowledgements

The authors are grateful to Bhagawan Sri Sathya Sai Baba, Founder Chancellor, SSSIHL, for His constant inspiration. The authors thank Prof. Olof Radmark, Karolinska Institute, Stockholm, Sweden for the gift of pT3 5-LOX plasmid. Shweta Sinha (SR/WOS-A/CS-126/2013) acknowledges the WOS-A, DST, GoI for funding and a fellowship.

References

1 R. Medzhitov, *Nature*, 2008, **454**, 428.
2 R. Gupta, D. P. Jindal and G. Kumar, *Bioorg. Med. Chem.*, 2004, **12**, 6331–6342.
3 D. A. Medina-Tato, M. L. Watson and S. G. Ward, *Drug Discovery Today*, 2006, **11**, 866–879.
4 W. Berger, M. De Chandt and C. Cairns, *Int. J. Clin. Pract.*, 2007, **61**, 663–676.
5 B. Fitzsimmons and J. Rokach, *Leukotrienes and lipoxygenases: chemical, biological, and clinical aspects*, Elsevier, Amsterdam, 1989, pp. 427–502.
6 M. Peters-Golden and W. R. Henderson Jr, *N. Engl. J. Med.*, 2007, **357**, 1841–1854.
7 C. Pergola and O. Werz, *Expert Opin. Ther. Pat.*, 2010, **20**, 355–375.

8 J. Y. Park, M. H. Pillinger and S. B. Abramson, *Clin. Immunol.*, 2006, **119**, 229–240.
9 D. Wang and R. N. DuBois, *Gut*, 2006, **55**, 115–122.
10 T. Båge, A. Kats, B. S. Lopez, G. Morgan, G. Nilsson, I. Burt, M. Korotkova, L. Corbett, A. J. Knox and L. Pino, *Am. J. Pathol.*, 2011, **178**, 1676–1688.
11 R. Nasrallah, R. Hassouneh and R. L. Hébert, *J. Am. Soc. Nephrol.*, 2016, **27**, 666–676.
12 K. Larsson, A. Kock, H. Idborg, M. A. Henriksson, T. Martinsson, J. I. Johnsen, M. Korotkova, P. Kogner and P.-J. Jakobsson, *Proc. Natl. Acad. Sci. U. S. A.*, 2015, **112**, 8070–8075.
13 H.-H. Chang and E. J. Meuillet, *Future Med. Chem.*, 2011, **3**, 1909–1934.
14 A. Koeberle, U. Siemoneit, U. Bühring, H. Northoff, S. Laufer, W. Albrecht and O. Werz, *J. Pharmacol. Exp. Ther.*, 2008, **326**, 975–982.
15 J. N. Dulin, M. L. Moore and R. J. Grill, *J. Neurotrauma*, 2013, **30**, 211–226.
16 Z. Pan, C. Chen, Y. Zhou, F. Xu and Y. Xu, *Drug Dev. Res.*, 2016, **77**, 43–49.
17 P. K. Sahu, *Eur. J. Med. Chem.*, 2016, **121**, 510–516.
18 Y. Wang, C. Yu, Y. Pan, X. Yang, Y. Huang, Z. Feng, X. Li, S. Yang and G. Liang, *Inflammation*, 2012, **35**, 594–604.
19 G. Liang, X. Li, L. Chen, S. Yang, X. Wu, E. Studer, E. Gurley, P. B. Hylemon, F. Ye and Y. Li, *Bioorg. Med. Chem. Lett.*, 2008, **18**, 1525–1529.
20 G. Liang, S. Yang, H. Zhou, L. Shao, K. Huang, J. Xiao, Z. Huang and X. Li, *Eur. J. Med. Chem.*, 2009, **44**, 915–919.
21 C. Zhao, Y. Cai, X. He, J. Li, L. Zhang, J. Wu, Y. Zhao, S. Yang, X. Li and W. Li, *Eur. J. Med. Chem.*, 2010, **45**, 5773–5780.
22 N. S. K. Reddy, R. Badam, R. Sattibabu, M. Molli, V. S. Muthukumar, S. S. S. Sai and G. N. Rao, *Chem. Phys. Lett.*, 2014, **616**, 142–147.
23 B. Rajashekar, P. Sowmendran, S. S. S. Sai and G. N. Rao, *J. Photochem. Photobiol., A*, 2012, **238**, 20–23.
24 M. S. Kiran, B. Anand, S. S. S. Sai and G. N. Rao, *J. Photochem. Photobiol., A*, 2014, **290**, 38–42.
25 M. J. Frisch, G. W. Trucks, H. B. Schlegel, G. E. Scuseria, M. A. Robb, J. R. Cheeseman, G. Scalmani, V. Barone, B. Mennucci and G. A. Petersson, *et al.*, *Gaussian09*, Gaussian. Inc., Wallingford CT, 2009, **121**, 150–166.
26 M. Hongbao, J. Young and C. Shen, *Nat. Sci.*, 2008, **6**, 66–75.
27 M. Ramanan, S. Sinha, K. Sudarshan, I. S. Aidhen and M. Doble, *Eur. J. Med. Chem.*, 2016, **124**, 428–434.
28 Y. Y. Zhang, O. Rådmark and B. Samuelsson, *Proc. Natl. Acad. Sci. U. S. A.*, 1992, **89**, 485–489.
29 L. Fischer, D. Szellas, O. Rådmark, D. Steinhilber and O. Werz, *FASEB J.*, 2003, **17**, 949–951.
30 P. Sivakumar, P. Prabhakar and M. Doble, *Med. Chem. Res.*, 2011, **20**, 482–492.
31 N. T. Smart, Version 6.28a, Bruker Analytical X-ray Systems, Inc., Madison, WI, 1998; SAINT Version 5.625, Bruker Analytical X-ray Systems, Inc. Madison, WI, 2001.
32 G. M. Sheldrick, SHELXS97 and SHELXL version 2014/7, http://shelx.uni-ac.gwdg.de/SHELX/index.php.
33 S. Sondhi, S. Rajvanshi, N. Singh, S. Jain and A. Lahoti, *Open Chem.*, 2004, **2**, 141–187.
34 A. Koeberle, E.-M. Haberl, A. Rossi, C. Pergola, F. Dehm, H. Northoff, R. Troschuetz, L. Sautebin and O. Werz, *Bioorg. Med. Chem.*, 2009, **17**, 7924–7932.
35 A. L. Blobaum and L. J. Marnett, *J. Biol. Chem.*, 2007, **282**, 16379–16390.
36 J. Habicht and K. Brune, *J. Pharm. Pharmacol.*, 1983, **35**, 718–723.
37 P.-J. Jakobsson, S. Thorén, R. Morgenstern and B. Samuelsson, *Proc. Natl. Acad. Sci. U. S. A.*, 1999, **96**, 7220–7225.
38 P. Moser, A. Sallmann and I. Wiesenberg, *J. Med. Chem.*, 1990, **33**, 2358–2368.
39 X. Laval, J. Delarge, F. Somers, P. d. Tullio, Y. Henrotin, B. Pirotte and J.-M. Dogne, *Curr. Med. Chem.*, 2000, **7**, 1041–1062.
40 F. Rörsch, E. l. Buscató, K. Deckmann, G. Schneider, M. Schubert-Zsilavecz, G. Geisslinger, E. Proschak and S. Grösch, *J. Med. Chem.*, 2012, **55**, 3792–3803.
41 M. Khoshneviszadeh, O. Shahraki, M. Khoshneviszadeh, A. Foroumadi, O. Firuzi, N. Edraki, H. Nadri, A. Moradi, A. Shafiee and R. Miri, *J. Enzyme Inhib. Med. Chem.*, 2016, **31**, 1602–1611.
42 M. Barone, G. Pannuzzo, A. Santagati, A. Catalfo, G. De Guidi and V. Cardile, *Molecules*, 2014, **19**, 6106–6122.
43 R. N. Young, *Eur. J. Med. Chem.*, 1999, **34**, 671–685.
44 S. Sinha, T. Sravanthi, S. Yuvaraj, S. Manju and M. Doble, *RSC Adv.*, 2016, **6**, 19271–19279.